peptides in $CHCl_3$ solvents cannot be done successfully due to solvent interference in the far-UV. Our goal in this work is to develop the basis set of conformationally characteristic peptide spectra for the newest technique, VCD, to a level where it will truly develop into a practical tool.

Acknowledgment. We thank the National Institutes of Health (Grant GM-30147, T.A.K.) for partial support of this research and the Research Board of the University of Illinois for partial purchase of the FT-IR spectrometer.

Registry No. LA_2, 103003-66-3; ALA_2, 103003-67-4; A_2LA_2, 103003-68-5; A_3LA_2, 103003-69-6; A_4LA_2, 103003-70-9; A_5LA_2, 100817-47-8.

On the Addition of Silyl Radicals to Unsaturated Carbonyl Compounds: Regioselectivity of the Attack and 1,3 Carbon to Oxygen Silicon Migration

Angelo Alberti,*† Chryssostomos Chatgilialoglu,† Gian Franco Pedulli,*‡ and Paolo Zanirato§

Contribution from the Istituto dei Composti del Carbonio Contenenti Eteroatomi e loro Applicazioni, CNR, 40064 Ozzano Emilia, Italy, Istituto di Chimica Organica dell'Universita', 40136 Bologna, Italy, and Istituto di Chimica Organica dell' Universita', 09100 Cagliari, Italy.
Received January 22, 1986

Abstract: The addition reactions of silyl radicals with 2,6-di-*tert*-butyl- (**1**), 2,6-dimethoxy- (**2**), and 2,6-dimethyl-*p*-benzoquinone (**3**), 3,6-dimethylthieno[3,2-*b*]thiophene-2,5-dione (**4**), 9-methyleneanthrone (**5**), and 5-benzylidene-3,6-dimethylthieno[3,2-*b*]thiophen-2-one (**6**) have been studied by EPR spectroscopy. With substrates **5** and **6** only the adducts resulting from attack at the exocyclic olefinic double bond were detected up to 400 K. With the quinones and dithiolactone **4** the nature of the adducts depended on the experimental temperature: thus at low temperature preferential addition of silyls to the less hindered ring carbon atom was evident, while at higher temperature only the adducts to a carbonyl oxygen were detected. Experimental evidence has been obtained that the kinetically favored carbon adduct converts to the thermodynamically more stable oxygen adduct via a 1,3 carbon to oxygen internal migration of the organometallic group involving a four-membered cyclic transition state. The kinetics of the rearrangement has been followed for the triphenylsilyl adduct of **1** and the Arrhenius equation $\log (k/s^{-1}) = [(13.8 \pm 0.3) - (18.2 \pm 0.3)]/\theta$ was determined. The rearrangement of the corresponding adduct of **4** was much slower and its kinetic analysis was complicated by a fast equilibration with its dimer. A kinetic scheme is outlined according to which the observed rate constants should refer to the rearrangement of the dimer rather than of the radical. An alike behavior is also reported for the triphenylgermyl adducts of compounds **1** and **4**.

It is well established that for molecules undergoing radical addition and containing both olefinic and carbonylic double bonds the preferred site of attack by carbon-centered radicals is the weaker C=C (πBDE[1] ca. 60 kcal/mol) rather than the C=O bond which is some 15 kcal/mol stronger.[2] Silyl radicals, in view of the exothermicity of their reactions with unsaturated derivatives, should attack preferentially C=C double bonds. Actually, in recent kinetic investigations, Ingold and co-workers showed that the rates of addition of trialkylsilyl radicals to olefins (ca. 10^6 to 10^7 M^{-1} s^{-1})[3] were about an order of magnitude higher than those for the addition to structurally related ketones (ca. 10^5 to 10^6 M^{-1} s^{-1}).[4]

Indeed, the low-temperature reaction of silyl radicals with isopropenyl acetate[5] or maleic anhydride[6] led to the EPR detection of species resulting from the addition to the olefinic double bonds; yet, in the large majority of reactions between silyls and unsaturated carbonyl compounds, only addition to C=O double bonds was observed.[7] Although the preferential formation of oxygen adducts was justified[7a] on thermodynamic basis with the greater strength of the O–Si bond thus formed (119–128 kcal/mol)[8,9] if compared with that of the C–Si bond (89 kcal/mol),[9] it remains in contradiction with expectation. This behavior can, however, be accounted for by two alternative reaction pathways involving as a first step the kinetically favored addition of $R_3Si^\bullet$ to the C=C double bond. Subsequently, the so formed primary radicals may evolve to the thermodynamically more stable oxygen adducts either by cleavage of the C–Si bond followed by readdition to the carbonyl group or by an intramolecular carbon to oxygen migration of silicon through a cyclic transition state. The former mechanism implies reversibility of the addition of silyls to unsaturated carbons which is known to be unimportant for the adducts to simple olefins.[10] The latter mechanism seems more reasonable in view

† Istituto CNR, Ozzano Emilia.
‡ Universita' di Cagliari.
§ Universita' di Bologna.

(1) (a) Citterio, A.; Minisci, F.; Vismara, E. *J. Org. Chem.* **1982**, *47*, 81–88. (b) Giese, B.; Kretzschmar, G. *Chem. Ber.* **1982**, *115*, 2012–2014 and references cited.
(2) Golden, D. M.; Benson, S. W. *Chem. Rev.* **1969**, *69*, 125.
(3) Chatgilialoglu, C.; Ingold, K. U.; Scaiano, J. C. *J. Am. Chem. Soc.* **1983**, *105*, 3292–3296.
(4) Chatgilialoglu, C.; Ingold, K. U.; Scaiano, J. C. *J. Am. Chem. Soc.* **1982**, *104*, 5119–5123.
(5) Bowles, A. J.; Hudson, A.; Jackson, R. A. *J. Chem. Soc. B* **1971**, 1947–1949.
(6) Alberti, A.; Hudson, A.; Pedulli, G. F. *Tetrahedron* **1982**, *38*, 3749–3752.
(7) (a) Cooper, J.; Hudson, A.; Jackson, R. A. *J. Chem. Soc., Perkin Trans. 2* **1973**, 1933–1937. (b) Alberti, A.; Hudson, A. *J. Chem. Soc., Perkin Trans. 2* **1978**, 1098–1102. (c) Chen, K. S.; Foster, T.; Wan, J. K. S. *Ibid.* **1979**, 1288–1292. (d) Adeleke, B. B.; Wan, J. K. S., *Ibid.* **1980**, 225–228. (e) Alberti, A.; Hudson, A.; Pedulli, G. F.; Zanirato, P. *J. Organomet. Chem.* **1980**, *198*, 145–154.
(8) Jackson, R. A. *Spec. Publ.—Chem. Soc.* **1970**, *No. 24*, 295–321.
(9) Walsh, R. *Acc. Chem. Res.* **1981**, *14*, 246–252.
(10) (a) Bennett, S. W.; Eaborn, C.; Jackson, R. A.; Pearce, R. *J. Organomet. Chem.* **1968**, *15*, P17–P17. (b) Jackson, R. A. *J. Chem. Soc., Chem. Commun.* **1974**, 573–574. (c) Chatgilialoglu, C.; Woynar, H.; Ingold, K. U.; Davies, A. G. *J. Chem. Soc., Perkin Trans. 2* **1983**, 555–561.

0002-7863/86/1508-4993$01.50/0

of the ability of β-keto silanes to thermally rearrange to siloxyalkenes, although such rearrangements have been reported to generally occur at rather high temperatures ($T > 100$ °C).[11] (The 1,3-silicon migration has been noted to occur at temperatures below 100 °C in the mass spectrometer.[11g])

The failure, with few exceptions, to detect silyl adducts to carbon can be reconciled with the rearrangement hypothesis if the silicon migration is significantly faster than in β-keto silanes. These carbon adducts would then be only detectable at low temperature whereas the rearranged species, i.e., the more stable oxygen adducts, would be observable at higher temperature. As most of the EPR investigations have been carried out at or above room temperature,[7b-e] it is possible that the primary spin adducts have been overlooked. A typical example, where either of the two isomeric adducts have been detected at different temperatures, is provided by the addition reaction of silyl or germyl radicals to maleic anhydride.[6]

We report here EPR evidence that silyls react with unsaturated carbonyl compounds by attacking preferentially the olefinic double bond. When addition occurs at a carbon β to oxygen, 1,3-migration of the silyl group takes place with rates strongly dependent on the nature of the substrate; no rearrangement occurs even at high temperatures when the silyl adds to a carbon more distant from the carbonyl oxygen.

Some results indicate that similar behavior is also exhibited by germyl radicals.

Experimental Section

The quinones and quinonoid compounds used as substrates for the addition of $Et_3Si^•$, $Ph_3Si^•$, and $Ph_3Ge^•$ radicals included the commercially available 2,6-di-*tert*-butyl- (**1**), 2,6-dimethoxy- (**2**), and 2,6-dimethyl-*p*-benzoquinone (**3**), 3,6-dimethylthieno[3,2-*b*]thiophene-2,5-dione (**4**),[12] 9-methylenanthrone (**5**),[13] and 5-benzylidene-3,6-dimethylthieno[3,2-*b*]thiophen-2-one (**6**),[14] which have been synthesized according to established methods.

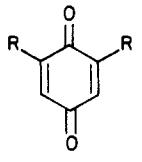

1, R = *t*-Bu
2, R = OMe
3, R = Me

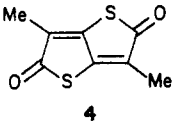

4

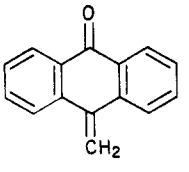

5

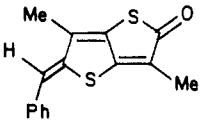

6

Radicals were generated by photolyzing nitrogen-purged benzene, *tert*-butylbenzene, or toluene solutions of the appropriate carbonyl substrate containing the group IVB (group 14)[21] metal hydride and di-*tert*-butyl peroxide. The light from a 1-kW high-pressure mercury lamp was filtered through a $CoSO_4$ (0.21 M)-$NiSO_4$ (1.14 M) aqueous solution. The temperature of the sample was controlled by means of standard devices and measured with a chromel–allumel thermocouple. EPR spectra were recorded on a Bruker ER 200 spectrometer.

The initial radical concentration was determined by double integration of the EPR signal and by comparison with the signal from a standard benzene solution of DPPH. The decay traces were either monitored directly on the spectrometer recorder or accumulated by means of an ASPECT 2000 dedicated computer.

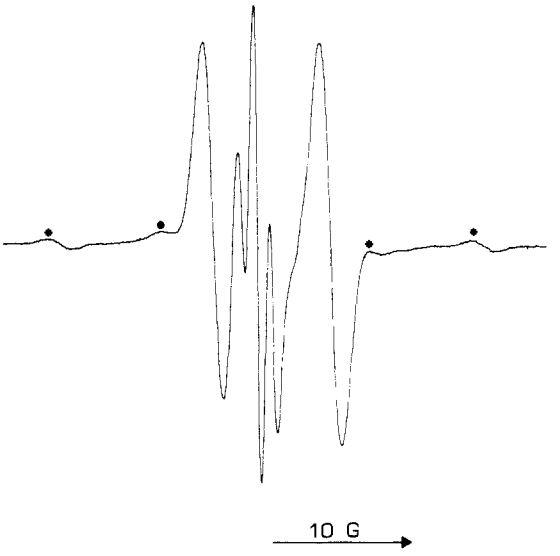

Figure 1. EPR spectrum observed at 225 K when reacting $Ph_3Si^•$ radicals with 2,6-di-*tert*-butyl-*p*-benzoquinone in *tert*-butylbenzene. Starred lines are ^{29}Si satellites of the doublet spectrum.

Results and Discussion

Reactions of silyl and germyl radicals with 1–4. The reaction of $Ph_3Si^•$ with 2,6-di-*tert*-butyl-*p*-benzoquinone (**1**) in deoxygenated *tert*-butylbenzene led to different EPR spectra at different temperatures. Thus, for $T > 300$ K the previously reported spectrum[7c] of the adduct of oxygen **7b** consisting of a 1:2:1 triplet

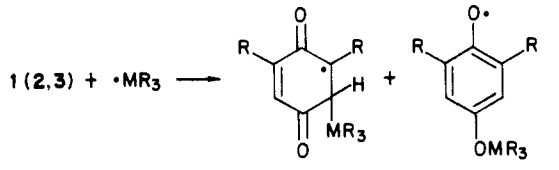

7a (8a, 9a) **7b (8b, 9b)**

was obtained. When the reaction was carried out below 300 K, a broad doublet (a_H 8.42 G), attributed to the ring adduct **7a**, became also detectable (Figure 1). The ratio between the two species was ca. 4:1 in favor of **7a** at 225 K. The somewhat small value of the doublet splitting is ascribed, as in the analogous diethoxyphosphonyl adducts of **1**,[15] to a distortion of the molecular framework compelling the β-proton close to the equatorial and the silicon atom close to the axial position. The significantly high value of the ^{29}Si coupling (22.0 G) suggests that this is indeed the case.

2,6-Dimethoxy-*p*-benzoquinone (**2**) behaved similarly when reacted with the organometallic radicals; at low temperature the EPR spectra showed the presence of both adducts (see Table I), whereas at 300 K only radical **8b** was detectable.

The addition of $Ph_3Si^•$ to quinone **3** at 230 K led to a weak spectrum consisting of a 1:3:3:1 quartet (22.66 G) of doublets (2.56 G) of doublets (1.57 G) centered at g 2.002 64. The magnitude of the quartet splitting might be consistent with structure **9a**, but the low values of the doublet splittings as well as of the g-factor cast serious doubts on this hypothetical assignment. At room or higher temperature the adduct to oxygen **9b** was instead easily detectable.

In the room temperature reaction of photogenerated triphenylsilyl radicals with 3,6-dimethylthieno[3,2-*b*]thiophene-2,5-dione (**4**), a spectrum was observed (Figure 2a) showing the

(11) (a) Brook, A. G. *Acc. Chem. Res.* **1974**, *7*, 77–84. (b) Brook, A. G.; MacRae, D. M.; Bassindale, A. R. *J. Organomet. Chem.* **1975**, *86*, 185–192. (c) Larson, G. L.; Fernandez, Y. V. *Ibid.* **1975**, *86*, 193–196. (d) Kwart, H.; Barnette, W. E. *J. Am. Chem. Soc.* **1977**, *99*, 614–616. (e) Kwart, H. *Phosphorus Sulfur* **1983**, *15*, 293–310. (f) Brook, A. G.; Bassindale, A. R. In *Rearrangements of Ground and Excited States*; de Mayo, P., Ed.; Academic Press: New York, 1980; Vol. 2, pp 149–227. (g) Tsai, R. S. C.; Larson, G. L.; Oliva, A. *Org. Mass Spectrom.* **1979**, *14*, 364–368.

(12) Martelli, G.; Testaferri, L.; Tiecco, M.; Zanirato, P. *J. Org. Chem.* **1975**, *40*, 3384–3391.

(13) de Barry Barnett, E.; Mattews, M. A. *Chem. Ber.* **1925**, *59*, 767.

(14) Testaferri, L.; Tiecco, M.; Zanirato, P. *J. Org. Chem.* **1975**, *40*, 3392–3395.

(15) Alberti, A.; Hudson, A.; Pedulli, G. F.; McGimpsey, W. G.; Wan, J. K. S. *Can. J. Chem.* **1985**, *63*, 917–921.

Table I. EPR Parameters for Radicals **7–12** Measured in Benzene or *tert*-Butylbenzene Solutions

radical	MR_3	T/K	hfs constants/G	g
7a	$SiPh_3$	225	8.42 (1 H), 22.00 (^{29}Si)	2.0041
	$SiEt_3$	203	6.93	2.0041
	$GePh_3$	203	7.95	2.0044
7b	$SiPh_3$	298	1.15 (2H)	2.0047
	$SiEt_3$[a]	298	0.97	2.0047
	$GePh_3$[a]	293	0.88, 1.15 (^{73}Ge)	2.0048
8a	$SiPh_3$	225	15.73 (1 H), 2.82 (3 H)	
8b	$SiPh_3$	296	1.11 (6 H)	2.0049
9b	$SiPh_3$	296	1.19 (2 H), 5.63 (6 H)	2.0049
10a	$SiPh_3$	298	8.31 (Me_6), 12.26 (^{29}Si)	2.0034
	$SiEt_3$	298	8.21	2.0034
	$GePh_3$	298	8.19	2.0035
10b	$SiPh_3$	350	1.16 (Me_3), 8.11 (Me_6), 3.10 (^{29}Si)	2.0034
	$SiEt_3$	340	1.09, 7.98	2.0034
	$GePh_3$	335	0.94, 7.75, 2.28 (^{73}Ge)	2.0033
11a	$SiPh_3$	298	2.80 ($H_{1,8}$), 0.88 ($H_{2,4,5,7}$), 3.15 ($H_{3,6}$), 8.55 (CH_2)	2.0033
	$GePh_3$	298	2.75, 0.88, 3.10, 8.05	2.0034
12a	$SiPh_3$	383	8.65 (Me_3), 1.53 (Me_6), 2.64 (CH)	2.0034
	$GePh_3$	363	8.60, 1.51, 2.81	2.0034

[a] In toluene.

simultaneous presence of two persistent radicals in different concentrations. The spectral pattern did not change with time or by interrupting the irradiation and resulted to be the combination of a 1:3:3:1 quartet (a_H 8.31 G) and of a weaker 1:3:3:1 quartet (a_H 8.11 G) of quartets (again 1:3:3:1, a_H 1.16 G). These two radicals were respectively identified as the ring (**10a**) and the oxygen (**10b**) adducts of $Ph_3Si^•$ with **4**. This assignment follows

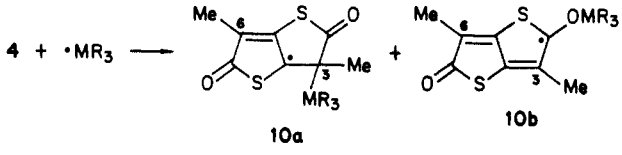

from the similarity of the proton splittings with those of the related diethoxyphosphonyl adducts of **4**, where the ^{31}P couplings (41.01 and 6.21 G, respectively)[15] allow a clear discrimination between the two radical species. When the same reaction was carried out above 360 K, radical **10b** became dominant and, as previously reported,[7e] was the only observable species after cutting off the light.

Similar results were obtained when reacting **4** with $Et_3Si^•$ and $Ph_3Ge^•$ radicals (see Table I).

The detection of different organometallic adducts from **1**, **2**, and **4** at different temperatures recalls what was previously found with maleic anhydride and related compounds.[6] As pointed out in the introduction, the conversion of the ring to the oxygen adducts may be the result either of the reversibility of the addition of silyl or germyl radicals to a C=C bond of the quinones or of an internal rearrangment of the primary adducts. Evidence favoring the latter mechanism was provided by the following two experiments. The adducts from **4** were generated at room temperature, the light was switched off, and the temperature was raised above 340 K. A sharp increase of the height of the signals together with a gradual variation of the ratio of the two species was observed, the total integrated intensity of the two spectra remaining practically

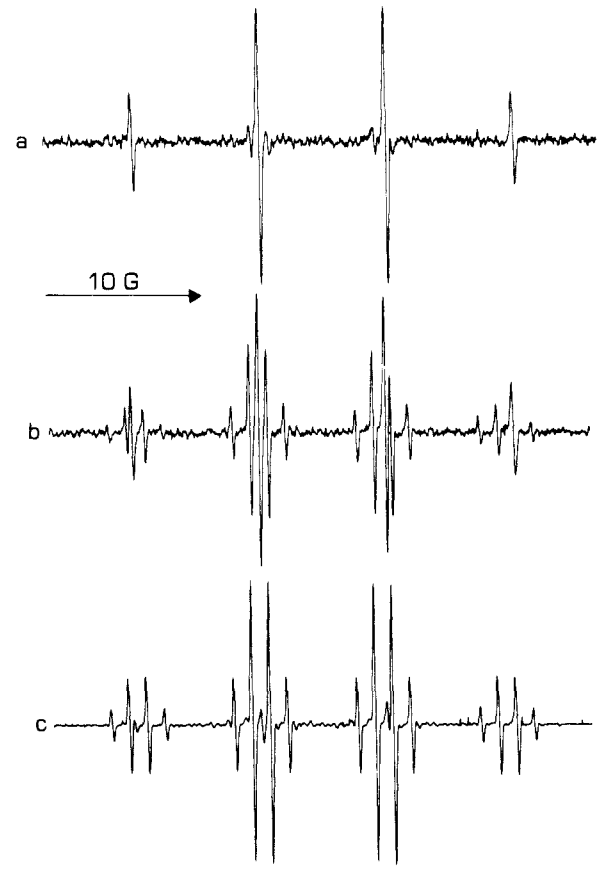

Figure 2. EPR spectra of the radicals obtained by reacting triphenylsilyl radicals with compound **4** recorded in *tert*-butylbenzene in the absence of light. (a) Room temperature spectrum; (b) spectrum at 325 K of a sample warmed for a few minutes at 350 K; (c) spectrum at 350 K after some time.

constant since the progressive decrease of the signals from **10a** was paralleled by an alike growth of those from **10b**. Once **10a** had completely disappeared, **10b** remained the only detectable species even upon cooling the solution, this indicating that **10a** transformed to **10b** *quantitatively and irreversibly*, the two radicals being characterized by almost identical free energies of dimerization. In the event that the conversion proceeded via cleavage of the carbon–silicon bond and readdition of $Ph_3Si^•$ to the oxygen atom, the yield for the transformation of **10a** to **10b** is not expected to be quantitative because of radical escape from the solvent cage. Moreover, one should be able to trap the intermediate organometallic radical with a suitable scavenger; we therefore repeated the temperature-jump experiment after adding to the solutions of the two adducts 1,3,5-trinitrobenzene, which is one of the most efficient spin traps for silicon-centered radicals:[16] However, no trace amounts of the expected silyloxy nitroxide were detected nor was the conversion of **10a** to **10b** affected. Instead, 3,5-dinitrophenyltriphenylsiloxy nitroxide was immediately formed by resuming irradiation, i.e., by producing new triphenylsilyl radicals.

Attempts to trap silyl radicals with trinitrobenzene also failed when substituting the quinone **1** for **4** in the system, in the temperature range where the isomerization of **7a** to **7b** could be monitored.

With the aim to further confirm the rearrangement mechanism, we generated at different temperatures the silyl and germyl radical adducts of 9-methyleneanthrone (**5**) and 5-benzylidene-3,6-dimethylthieno[3,2-*b*]thiophen-2-one (**6**) where the initial addition was expected to occur at the exocyclic C=C double bond. Since no particular structural requirement has to be met for the cleavage–readdition process to take place, whereas the rear-

(16) Alberti, A.; Degl'Innocenti, A.; Pedulli, G. F.; Ricci, A. *J. Am. Chem. Soc.* **1985**, *107*, 2316–2319.

rangement can only occur if the formation of a cyclic transition state is possible, conversion of the carbon to the oxygen adducts of **5** and **6**, if observed, would provide evidence in favor of the former mechanism.

Reactions of Silyl and Germyl Radicals with 5 and 6. The room temperature reaction of Ph_3Si radicals with 9-methyleneanthrone (**5**) in deoxygenated *tert*-butylbenzene solutions led to a strong EPR spectrum characteristic of a single radical adduct, which was interpreted on the basis of the hyperfine splitting (hfs) constants reported in Table I. Raising the temperature up to 400 K produced an enhancement of the spectral lines and minor variations in the proton couplings but did not result in the appearance of other radical species. Similar results were obtained when using triphenylgermane (see Table I).

The addtion of an organometallic radical, $R_3M^\bullet$, to **5** may give rise to the two adducts **11a** and **11b** formed by attack at either

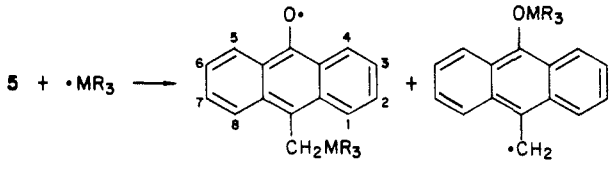

11a **11b**

the methylenic carbon or the carbonyl oxygen, respectively. We assign structure **11a** to the observed radicals because (i) the adducts show a rather high persistence, unexpected for benzyl-like radicals but in line with that of other aroxyls, (ii) the *g* factors (ca. 2.0034) are indicative of aroxyls rather than of carbon-centered radicals, and (iii) the proton hfs constants are close to those of the adducts between **5** and carbon- or sulfur-centered radicals.[17]

Only one radical species was also obtained in the temperature range 300–400 K when reacting compound **6** with silyls or germyls. The EPR spectral parameters collected in Table I are consistent with structure **12a** rather than **12b** since the phenyl ring protons

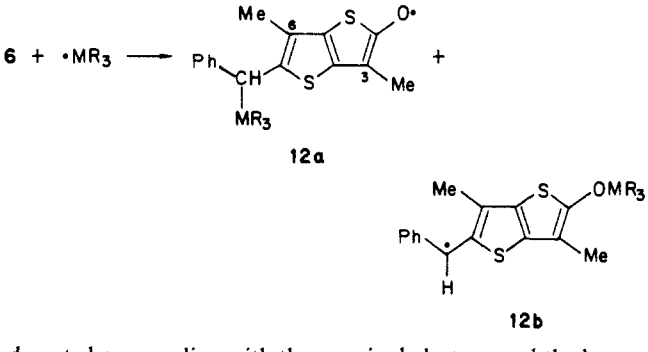

12a

12b

do not show coupling with the unpaired electron and the benzylidenic proton splitting (ca. 2.7 G) is much smaller than expected for a diarylmethyl radical (e.g., 14.7 G for $Ph_2C^\bullet H$).[18]

We therefore conclude that not only silyl (or germyl) radicals attack preferentially olefinic with respect to C=O double bonds but also that conversion of carbon to oxygen adducts takes place, at temperatures <400 K, only if the group IVB (group 14) metal is linked to a carbon adjacent to the carbonyl group.

Kinetics of the Rearrangment Reactions. Having estabilished that the initially formed ring adducts of silyls with quinones convert to the thermodynamically more stable adducts to oxygen via a rearrangement reaction, the kinetics of the process was investigated in the case of **7a** and **10a** with $R_3M = Ph_3Si$.

Since these radicals are in equilibrium with their dimers, all the possible reactions that may take place in this system have to be considered as shown in Scheme I, where A• and B• represent the unrearranged and the rearranged radicals, respectively.

According to this scheme radical A• may decay either by direct rearrangement to B• with rate constant *k* or by dimerization to

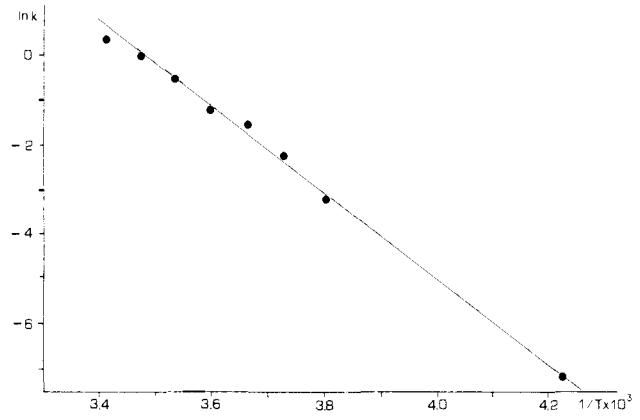

Figure 3. Arrhenius plot for the first-order rate constant of the rearrangement of **7a** to **7b** ($R_3M = Ph_3Si$).

Scheme I

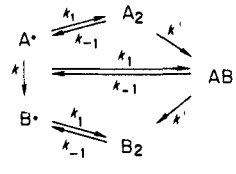

A_2 which in turn can rearrange to AB. The latter species either dissociates into A• and B• or further rearranges to B_2 which may again dissociate into B•.

Scheme I relies on the following assumptions which will be justified further on: (i) Radicals A• and B• do not decay via other mechanisms; i.e., at a given temperature eq 1 holds, where the

$$[A^\bullet]_t + [B^\bullet]_t = [A^\bullet]_0 \quad (1)$$

subscripts refer to time zero and *t*. (ii) The equilibrium constants for dissociation, $k_{-1}/k_1 = 1/K_{eq}$, of A_2, AB, and B_2 are the same. (iii) Dimers A_2 and AB rearrange to AB and B_2, respectively, with the same rate constant k'.

This scheme could be considerably simplified with the adducts of 2,6-di-*tert*-butyl-*p*-benzoquinone (**1**) since radicals **7a** and **7b** were remarkably persistent with respect to dimerization. In fact, when stopping the UV irradiation, no decay was observed below 220 K while **7b** decayed to the equilibrium concentration with a half-time of the order of minutes at 300 K. All reactions other than (2) were therefore neglected. The decay traces of **7a** ob-

$$A^\bullet \xrightarrow{k} B^\bullet \quad (2)$$

served when cutting off the light were actually clean first order in the temperature range 260–290 K. Above 300 K the EPR signals of **7a** were too weak to follow the rearrangement, while below 250 K the decay traces departed from first order because isomerization and dimerization had comparable rates. However, an estimate of the rate of rearrangement could be obtained also at 235 K by monitoring the variations of the ratio of the structural isomers with time on the assumption that both **7a** and **7b** dimerized with the same second-order rate constant. The experimental results, as shown in Figure 3, nicely fitted an Arrhenius plot which provided the following activation parameters: log (A/s^{-1}) 13.8 ± 0.3, E_a 18.2 ± 0.3 kcal/mol.

With the adduct of the dithiolactone **4** the situation was rather more complicated. Radical **10a** ($R_3M = Ph_3Si$) did not significantly rearrange below 340 K and when cutting off the light its concentration rapidly decreased to the equilibrium value due to dimerization. Scheme I had therefore to be used for the kinetic analysis. For the couple of radicals **10a** and **10b** the first two assumptions implicit in Scheme I are fulfilled since the quantitative transformation of one into the other (vide supra), at a given temperature, demonstrates that the two radicals do not decay by other routes and that the equilibrium constants for the dissociation of A_2, AB, and B_2 are equal. Additional evidence concerning the

(17) Alberti, A.; Leardini, R.; Pedulli, G. F.; Tundo, A.; Zanardi, G. *Tetrahedron* **1986**, *42*, 2533–2538.

(18) Bassindale, A. R.; Bowles, A. J.; Hudson, A.; Jackson, R. A.; Schreiker, K.; Berndt, A. *Tetrahedron Lett.* **1973**, 3185–3186.

Table II. Observed First-Order Rate Constants for the Decay of **10a** to **10b** (R_3M = Ph_3Si) Measured at Different Initial Radical Concentrations $[A^\cdot]_0$ at 362 K

$[A^\cdot]_0 \times 10^7$/M	3.3	4.3	5.1	7.6	12.9	14.2	18.0	27.4
$k_{obsd} \times 10^3/s^{-1}$	4.8	11.4	6.1	6.5	7.7	6.1	3.1	4.2

latter point was obtained from the determination of the enthalpies of dimerization, ΔH, for radicals **10a** and **10b**. van't Hoff plots of the relative radical concentrations, corrected for the temperature dependence of the sensitivity of the EPR spectrometer, provided two practically identical values of ΔH, i.e. −26.8 and −26.3 kcal/mol for **10a** and **10b**, respectively, in the temperature range 310–360 K (a ΔH value of −13.1 kcal/mol was determined for radical **7b**). Assumption iii, implying that the structure for one-half of the dimer does not affect the rearrangement of the other half, could not be verified but appears quite reasonable.

According to Scheme I (see Appendix) the decay of **10a** should follow first-order kinetics with an observed rate constant given by eq 3. Three limiting cases can be envisaged for eq 3: (i) The

$$k_{obsd} = (k + 2k'K_{eq}[A^\cdot]_0)/(1 + 2K_{eq}[A^\cdot]_0) \quad (3)$$

rate of rearrangement for the radical, k, and the dimers, k', are the same. The observed rate constant, being

$$k_{obsd} = k = k' \quad (4)$$

is the true rate of rearrangment. (ii) $2K_{eq}[A^\cdot]_0 >> 1$; that is, the equilibrium is largely shifted toward the dimer, therefore

$$k_{obsd} = k' + k/(2K_{eq}[A^\cdot]_0) \quad (5)$$

A plot of k_{obsd} as a function of the reciprocal of the initial radical concentration, $1/[A^\cdot]_0$, should be linear and provide k' as intercept and $k/2K_{eq}$ as slope. (iii) $2K_{eq}[A^\cdot]_0 << 1$; that is, the equilibrium is shifted towards the monomer, therefore

$$k_{obsd} = k + 2k'K_{eq}[A^\cdot]_0 \quad (6)$$

A linear plot of k_{obsd} against $[A^\cdot]_0$ providing k and $2k'K_{eq}$ should be obtained.

The kinetic study for the rearrangement of **10a** to **10b** was carried out by using the following procedure. A typical sample was irradiated at room temperature until the signals from radical **10a** reached a plateau; irradiation was then interrupted and the EPR tube taken off the cavity. The temperature was then raised to the desired value and after stabilization the tube was reinserted. The signals from **10a** suddenly increased to reach the new equilibrium and then gradually decreased due to the rearrangement to **10b**.

Both the decay of the signals from **10a** and the growth of those from **10b** followed first-order kinetics and provided almost identical rate constants, k_{obsd}. A choice between eq 4, 5, or 6 for k_{obsd} is not straightforward. However, since the equilibrium constant, K_{eq}, at 360 K could be estimated to be of the order of 10^8 to 10^9 M^{-1} by using the measured ΔH for dimerization (ca. 26.5 kcal/mol) and a reasonable value, around −35 eu, for the corresponding ΔS,[19] even for the lower concentration of radical (3×10^{-7} M) used in our experiments, the condition $2K_{eq}[A^\cdot]_0 >> 1$ was satisfied. The last of the three above possibilities is therefore ruled out and the observed first-order rate constant will be given by either eq 4 or 5. To discriminate between these two cases many experiments have been run at a fixed temperature (362 K) and at different radical concentration $[A^\cdot]_0$. The observed rate constants reported in Table II show a scattering around the mean value of 6.2×10^{-3} s^{-1} without any apparent correlation with $[A^\cdot]_0$.

From these results it can be inferred that k_{obsd} represents the rate of rearrangement of the dimer, k', which may (eq 4) or may not coincide with that of the radical, k.

The rearrangement of **10a** (MR_3 = $SiPh_3$) was also studied at a few other temperatures. Since, however, the available range was rather small (345–362 K), the Arrhenius parameters could be determined with low accuracy. We therefore estimated the activation energy E_a as 26.5 kcal/mol by using k_{obsd} at 362 K and the log A value of 13.8 obtained for the rearrangement of **7a**.

The isomerization of **10a** to **10b** was also followed for R_3M = Et_3Si and Ph_3Ge, the observed rate constants being respectively 2.7×10^{-3} at 360 K and 1.44×10^{-3} s^{-1} at 355 K.

Conclusions

The above results indicate that the attack of silyl or germyl radicals to carbon–carbon double bonds of unsaturated carbonyl compounds is a more facile process than attack to carbon–oxygen double bonds even though the adducts resulting from the latter reaction are thermodynamically more stable. The preferential formation of the carbon adducts is likely to reflect the different activation energies for the two processes, being the preexponential factors determined by Ingold et al. for the addition of silyl radicals to either olefins[3] or carbonyl[4] groups, which are fairly similar, viz. ca. 10^9 M^{-1} s^{-1}. Within this assumption the activation energy for the addition of silyls to the C=C double bond of **1** can be calculated, from the ratio of the oxygen and of the ring adducts at 215 K, to be ca. 0.3 kcal/mol lower than that for the addition to C=O when correcting for the statistical factor; ΔE_a is similarly calculated as ca. 0.8 kcal/mol at 298 K in the case of **4**.

Once the carbon adducts had been formed, different behavior was observed depending on the relative position of the carbon bearing the organometallic substituent and the carbonyl oxygen. In the radicals from **5** and **6**, where these atoms are far apart, no isomerization was detected up to 400 K, while in all the adducts where initial addition occurred at a carbon atom α to the carbonyl group, rearrangement leading to the thermodynamically more stable oxygen adduct was observed. It would therefore appear that the formation of a four-membered cyclic transition state, as the one proposed in the thermal rearrangement of β-keto silanes,[11] is crucial for the carbon to oxygen silicon or germanium migration to take place. This behavior is also a clear indication of the nonhomolytic nature of this internal shift.

In the present cases, rearrangement occurred faster than with β-keto silanes. Since the preexponential factor for the rearrangement of **7a** (6.3×10^{13} s^{-1}) is very close to that reported by Kwart and Barnette[11d] for that of trimethylsilylacetophenone in benzene (8.89×10^{13} s^{-1}), the rate difference is explained by the lower activation energy, E_a, of the former reaction, i.e., 18.2 against 30.6 kcal/mol. It is conceivable that this significant difference is due to the fact that conversion of **7a** to **7b** is accompanied by aromatization of the six-membered ring although the paramagnetic nature of **7a** may also concur to a lowering of the activation energy. Consistently, the previously reported rearrangement of **13a** to **13b**,[20] where the migration of the silyl group also leads to aromatization, occurs at ordinary temperatures, that is, much more readily than that of β-keto silanes. The intermediate value of the activation energy for the rearrangement of **10a** (26.5 kcal/mol) can be rationalized on the same basis. In this case the energy gain is expected to be lower than with **7a** since aromatization of

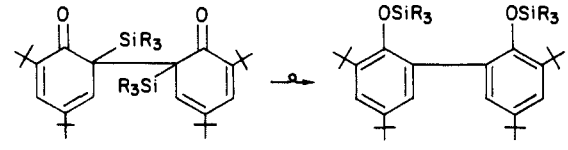

13a **13b**

R = Me

(19) Weiner, S. A.; Mahoney, L. R. *J. Am. Chem. Soc.* **1972**, *94*, 5029–5033.

(20) (a) Beckwith, A. L. J.; Ingold, K. U. In *Rearrangements in Ground and Excited States*; de Mayo, P., Ed.; Academic Press: New York, 1980; Vol. 1, pp 161–310. (b) Razuvaev, G. A.; Vasileskaja, N. S.; Muslin, D. V. *J. Organomet. Chem.* **1967**, *7*, 531–533.

(21) In this paper the periodic group notation in paranthesis is in accord with recent actions by IUPAC and ACS nomenclature committees. A and B notation is eliminated because of wide confusion. Groups IA and IIA become groups 1 and 2. The d-transition elements comprise groups 3 through 12, and the p-block elements comprise groups 13 through 18. (Note that the former Roman number designation is preserved in the last digit of the new numbering: e.g., III → 3 and 13.)

a condensed thiophen ring is involved.

Stereoelectronic effects might also be responsible for the lower activation energy for the rearrangement of **7a**, as the cleavage of the C_2–Si bond can be assisted by the interaction with the singly occupied $2p_z$ orbital on C_3. The radical geometry as inferred from the EPR parameters is such to maximize this interaction.

Acknowledgment. Financial support from "Progetto Finalizzato Chimica Fine e Secondaria" del CNR is gratefully acknowledged. We express our gratitude to Prof. E. Ciuffarin for discussions and helpful suggestions and to G. Bragaglia for his skillful technical assistance.

Appendix

The rates of decay of the unrearranged species, $-d[A^\bullet]/dt$, $-d[A_2]/dt$, and $-d[AB]/dt$ can be expressed as indicated in the following equations:

$$-d[A^\bullet]/dt = k[A^\bullet] + 2k_1[A^\bullet]^2 - 2k_{-1}[A_2] + 2k_1[A^\bullet][B^\bullet] - k_{-1}[AB] \quad (7)$$

$$-d[A_2]/dt = -k_1[A^\bullet]^2 + k_{-1}[A_2] + 2k'[A_2] \quad (8)$$

$$-d[AB]/dt = -2k_1[A^\bullet][B^\bullet] + k_{-1}[AB] + k'[AB] - 2k'[A_2] \quad (9)$$

If we now define $[A_T]$ as the total concentration of the unrearranged A, either as radical or dimer, i.e.,

$$[A_T] = [A^\bullet] + 2[A_2] + [AB] \quad (10)$$

the rate of disappearance of A_T is

$$-d[A_T]/dt = -d[A^\bullet]/dt - 2\,d[A_2]/dt - d[AB]/dt \quad (11)$$

or, by substituting eq 7–9 in eq 11,

$$-d[A_T]/dt = k[A^\bullet] + k'(2[A_2] + [AB]) \quad (12)$$

Condition ii implies that

$$K_{eq} = [A_2]/[A^\bullet]^2 = [B_2]/[B^\bullet]^2 = [AB]/(2[A^\bullet][B^\bullet]) \quad (13)$$

If we now further assume that the reaching of equilibrium is fast compared to the rearrangement of radical $[A^\bullet]$, i.e., $k_1[A^\bullet] >> k$, this seeming true below 370 K for **10a**, the last two terms of eq 11 can be expressed as

$$-2\,d[A_2]/dt = -2K_{eq}\,d[A^\bullet]^2/dt \quad (14)$$

$$-d[AB]/dt = 2K_{eq}\,d\{[A^\bullet]([A^\bullet]_0 - [A^\bullet])\}/dt = -2K_{eq}[A^\bullet]_0\,d[A^\bullet]/dt + 2K_{eq}\,d[A^\bullet]^2/dt \quad (15)$$

Equation 11 then becomes

$$-d[A_T]/dt = -(1 + 2K_{eq}[A^\bullet]_0)\,d[A^\bullet]/dt \quad (16)$$

Similarly, by substituting eq 13 into eq 12, we get

$$-d[A_T]/dt = (k + 2k'K_{eq}[A^\bullet]_0)[A^\bullet] \quad (17)$$

and by combining eq 16 and 17,

$$-d[A^\bullet]/dt = [A^\bullet](k + 2k'K_{eq}[A^\bullet]_0)/(1 + 2K_{eq}[A^\bullet]_0) \quad (18)$$

The decay of radical **10a** should then follow first-order kinetics, with

$$k_{obsd} = (k + 2\,k'K_{eq}[A^\bullet]_0)/(1 + 2K_{eq}[A^\bullet]_0) \quad (3)$$

independently of the relative values of k, k', and K_{eq}.

Registry No. **1**, 719-22-2; **2**, 530-55-2; **3**, 527-61-7; **4**, 60749-72-6; **5**, 4159-04-0; **6**, 56412-33-0; **7a** (MR_3 = $SiPh_3$), 102725-16-6; **7a** (MR_3 = $SiEt_3$), 102725-17-7; **7a** (MR_3 = $GePh_3$), 102725-18-8; **7b** (MR_3 = $SiPh_3$), 72975-18-9; **7b** (MR_3 = $SiEt_3$), 102725-19-9; **7b** (MR_3 = $GePh_3$), 102725-20-2; **8a** (MR_3 = $SiPh_3$), 102725-21-3; **8b** (MR_3 = $SiPh_3$), 87066-11-3; **9b** (MR_3 = $SiPh_3$), 73818-08-3; **10a** (MR_3 = $SiPh_3$), 102725-22-4; **10a** (MR_3 = $SiEt_3$), 102725-23-5; **10a** (MR_3 = $GePh_3$), 102725-24-6; **10b** (MR_3 = $SiPh_3$), 102725-25-7; **10b** (MR_3 = $SiEt_3$), 102725-26-8; **10b** (MR_3 = $GePh_3$), 102725-27-9; **11a** (MR_3 = $SiPh_3$), 102725-28-0; **11a** (MR_3 = $GePh_3$), 102725-29-1; **12a** (MR_3 = $SiPh_3$), 102725-30-4; **12a** (MR_3 = $GePh_3$), 102725-31-5; $Et_3Si^\bullet$, 24669-77-0; $Ph_3Si^\bullet$, 18602-99-8; $Ph_3Ge^\bullet$, 55321-79-4.

The Complex between Carboxypeptidase A and a Possible Transition-State Analogue: Mechanistic Inferences from High-Resolution X-ray Structures of Enzyme–Inhibitor Complexes

David W. Christianson† and William N. Lipscomb*

Contribution from the Gibbs Chemical Laboratories, Department of Chemistry, Harvard University, Cambridge, Massachusetts 02138. *Received December 27, 1985*

Abstract: The mode of binding of the competitive inhibitor 2-benzyl-4-oxo-5,5,5-trifluoropentanoic acid to the active site of carboxypeptidase A has been studied by X-ray diffraction methods to a resolution of 1.7 Å. The actual species bound to the enzyme is the *gem*-diol moiety resulting from covalent hydration at the ketone carbonyl. The observed structure of this enzyme–inhibitor complex provides one possible model for a tetrahedral intermediate that would be encountered in a promoted water/hydroxide hydrolytic mechanism. Additionally, this structure yields the first direct interaction of Arg-127 with a zinc-bound oxygen of an inhibitor. General mechanistic and structural inferences are drawn based upon the structures of this and other recently determined enzyme–inhibitor complexes. An important realization is that the actual catalytic route of the enzyme may proceed through a sequence of orientations of the tetrahedral intermediate(s). New structural features are discussed, including the change in the zinc coordination polyhedron and the catalytic importance of Arg-127.

The zinc protease carboxypeptidase A (CPA) is no stranger to debate[1-4] about its particular mechanism(s) in the hydrolysis of peptide or ester substrates (promoted water/hydroxide or anhydride pathways). The X-ray diffraction studies implicate Glu-270, Arg-127, Arg-145, Tyr-248, Zn^{2+}, and the zinc-bound

† AT&T Bell Laboratories Scholar.

(1) Lipscomb, W. N. *Acc. Chem. Res.* **1982**, *15*, 232–238.

0002-7863/86/1508-4998$01.50/0